Gata2 cis-element is required for hematopoietic stem cell generation in the mammalian embryo

Xin Gao,[1,3] Kirby D. Johnson,[1,3] Yuan-I Chang,[2,3] Meghan E. Boyer,[1,3] Colin N. Dewey,[4] Jing Zhang,[2,3] and Emery H. Bresnick[1,3]

[1]Department of Cell and Regenerative Biology, Carbone Cancer Center, and [2]McArdle Laboratory for Cancer Research, [3]UW-Madison Blood Research Program; and [4]Department of Biostatistics and Medical Informatics, University of Wisconsin School of Medicine and Public Health, Madison, WI 53705

The generation of hematopoietic stem cells (HSCs) from hemogenic endothelium within the aorta, gonad, mesonephros (AGM) region of the mammalian embryo is crucial for development of the adult hematopoietic system. We described a deletion of a *Gata2 cis*-element (+9.5) that depletes fetal liver HSCs, is lethal at E13–14 of embryogenesis, and is mutated in an immunodeficiency that progresses to myelodysplasia/leukemia. Here, we demonstrate that the +9.5 element enhances *Gata2* expression and is required to generate long-term repopulating HSCs in the AGM. Deletion of the +9.5 element abrogated the capacity of hemogenic endothelium to generate HSC-containing clusters in the aorta. Genomic analyses indicated that the +9.5 element regulated a rich ensemble of genes that control hemogenic endothelium and HSCs, as well as genes not implicated in hematopoiesis. These results reveal a mechanism that controls stem cell emergence from hemogenic endothelium to establish the adult hematopoietic system.

CORRESPONDENCE
Emery H. Bresnick:
ehbresni@wisc.edu

Abbreviations used: AGM, aorta, gonad, mesonephros; HSC, hematopoietic stem cell.

The paradigm for how the adult hematopoietic system emerges during mammalian embryogenesis involves a poorly understood hemogenic endothelium to hematopoietic stem cell (HSC) transition in the aorta, gonad, mesonephros (AGM) region (Dzierzak and Speck, 2008; Zovein et al., 2008; Bertrand et al., 2010; Boisset et al., 2010) This stem cell generation occurs within the E10.5–E12.5 AGM, and AGM-derived HSCs populate the fetal liver, rendering it the dominant hematopoietic site (Medvinsky et al., 1993; Medvinsky and Dzierzak, 1996). Conditional knockout studies indicate that the transcription factor Runx1 functions in hemogenic endothelium to promote HSC generation (Chen et al., 2009), and in an immortalized hematopoietic cell line, Runx1 co-occupies a large number of chromatin sites with other established regulators of hematopoiesis (Wilson et al., 2010). We reasoned that other master regulators function in concert with Runx1 in hemogenic endothelium, downstream of Runx1 in HSCs, or in both contexts. The critical regulator of hematopoiesis GATA-2 (Tsai et al., 1994), a member of the GATA transcription factor family (Bresnick et al., 2012), represents a prime candidate for controlling the hemogenic endothelium to HSC transition and/or subsequent HSC function. Targeted deletion of *Gata2* yields severe anemia and embryonic lethality at E10.5 (Tsai et al., 1994), with impaired function of *Gata2*$^{+/-}$ HSCs (Ling et al., 2004; Rodrigues et al., 2005) and granulocyte-macrophage progenitors (Rodrigues et al., 2008).

Given the GATA-2 activity to control hematopoiesis and many unanswered questions regarding when and how GATA-2 functions during embryogenesis, it is instructive to consider the molecular circuitry regulating *Gata2* expression. GATA-2 occupies five *Gata2* locus sites (−77, −3.9, −2.8, −1.8, and +9.5 kb relative to the 1S promoter transcription start site; Grass et al., 2006). GATA-1–mediated displacement of GATA-2 from these sites during erythropoiesis correlates with repression (Bresnick et al., 2010). Because it was unclear whether these sites mediate *Gata2* activation, repression, or both, and if they solely control *Gata2* expression in erythroid

The Rockefeller University Press $30.00
J. Exp. Med. 2013 Vol. 210 No. 13 2833-2842
www.jem.org/cgi/doi/10.1084/jem.20130733

The Journal of Experimental Medicine

cells, we generated mouse strains lacking the −2.8, −1.8, or +9.5 GATA switch sites. Although the −2.8 and −1.8 sites do not regulate HSC function (Snow et al., 2010, 2011), the +9.5 element, consisting of an E-box, spacer, and GATA motif, establishes fetal liver hematopoietic stem and progenitor cells (Fig. 1 A) and confers vascular integrity, but not yolk sac hematopoiesis (Johnson et al., 2012). Additional evidence supporting the importance of the +9.5 element emerged via conditional disruption of *Gata2* using a +9.5 element-driven Cre recombinase (Lim et al., 2012). However, mechanisms underlying +9.5 element function are not established.

Herein, we used the +9.5 element mutant strain to investigate the problem of how hemogenic endothelium in the AGM gives rise to HSCs. We demonstrate that the +9.5 element is required for the emergence of functional HSCs in the AGM and for hemogenic endothelium to generate HSC-containing c-Kit$^+$ cell clusters. Genomic analyses revealed that the +9.5 element establishes a genetic network in hemogenic endothelium involving known regulators of hemogenic endothelium and HSCs, as well as genes not implicated in hematopoiesis. These results support a model in which the +9.5 element instigates a complex genetic network in hemogenic endothelium, and the established regulator of the hemogenic endothelium to HSC transition *Runx1* (Chen et al., 2009) is one of the downstream components mediating the control of definitive hematopoiesis.

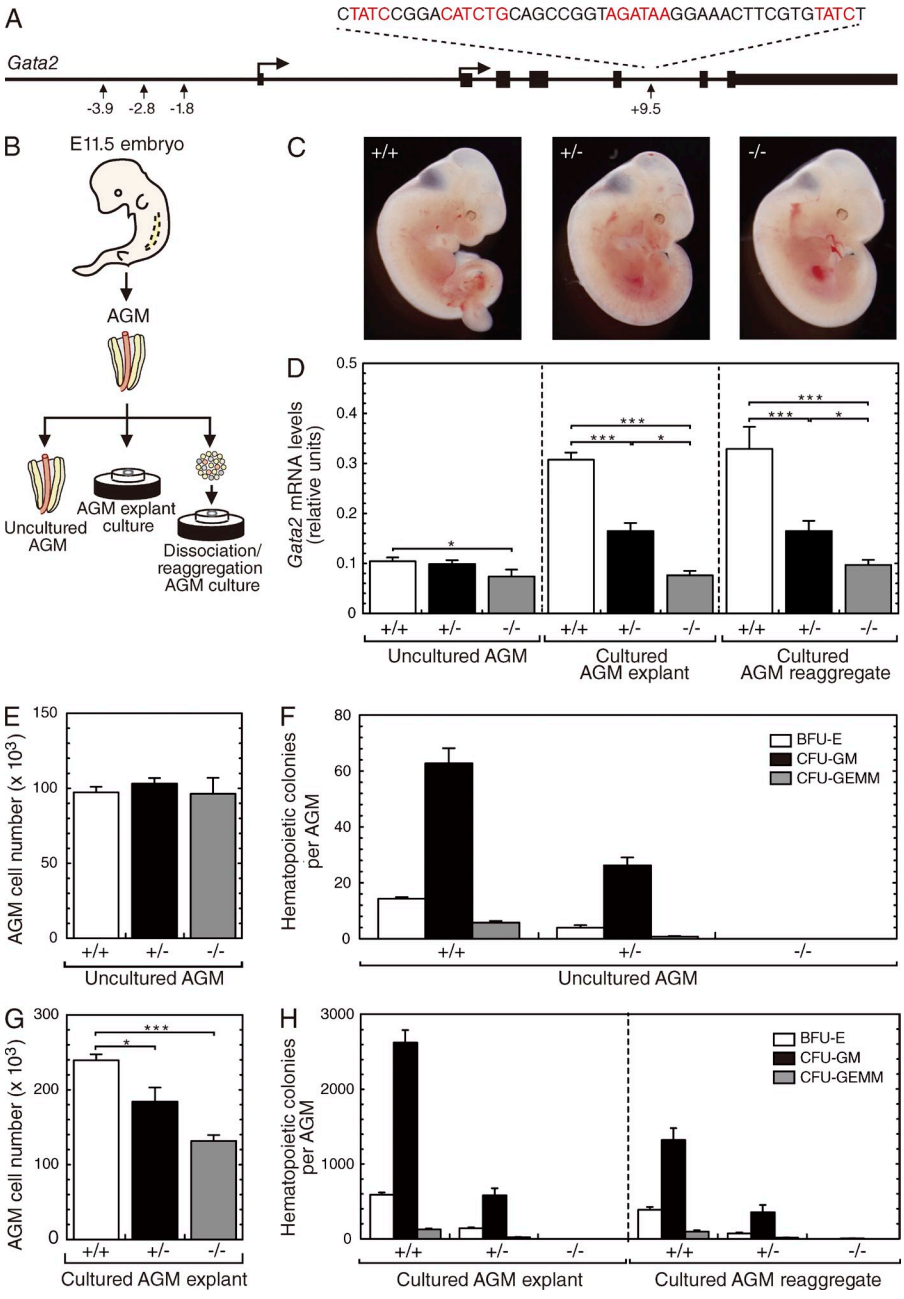

Figure 1. Cis-regulatory element requirement for *Gata2* expression and hematopoietic progenitor activity in the AGM. (A) Schematic diagram for targeted deletion of the E-box-GATA composite element in murine *Gata2* locus. (B) AGM ex vivo culture system. (C) Representative images of E11.5 +9.5$^{+/+}$,+9.5$^{+/-}$, and +9.5$^{-/-}$ embryos. (D) Real-time RT-PCR analysis of *Gata2* expression levels in E11.5 uncultured AGMs, cultured AGM explants, and cultured AGM reaggregates (4 independent experiments and 5 litters for uncultured AGMs: +9.5$^{+/+}$ [n = 13]; +9.5$^{+/-}$ [n = 18]; +9.5$^{-/-}$ [n = 7]; 2 independent experiments and 2 litters for cultured AGM explants: +9.5$^{+/+}$ [n = 5]; +9.5$^{+/-}$ [n = 13]; +9.5$^{-/-}$ [n = 3]; 5 independent experiments and 5 litters for cultured AGM reaggregates: +9.5$^{+/+}$ [n = 10]; +9.5$^{+/-}$ [n = 20]; +9.5$^{-/-}$ [n = 12]). (E and G) Quantitative analysis of cell number in E11.5 uncultured AGMs (E) and cultured AGM explants (G). (F and H) Quantitative analysis of colony-forming activity of hematopoietic progenitors in E11.5 uncultured AGMs (F), cultured AGM explants (H), and cultured AGM reaggregates (H; 2 independent experiments and 2 litters for uncultured AGMs: +9.5$^{+/+}$ [n = 5]; +9.5$^{+/-}$ [n = 10]; +9.5$^{-/-}$ [n = 4]; 2 independent experiments and 2 litters for cultured intact AGM explants: +9.5$^{+/+}$ [n = 5]; +9.5$^{+/-}$ [n = 5]; +9.5$^{-/-}$ [n = 3]; 2 independent experiments and 2 litters for cultured AGM reaggregates: +9.5$^{+/+}$ [n = 6]; +9.5$^{+/-}$ [n = 8]; +9.5$^{-/-}$ [n = 6]). All error bars represent SEM. *, P < 0.05; ***, P < 0.001 (two-tailed unpaired Student's t test).

RESULTS AND DISCUSSION

+9.5 element is essential for *Gata2* expression in the AGM

To investigate how a cis-regulatory element controls stem cell generation/function, we asked whether the fetal liver HSC deficiency is caused by defective HSC-generation in the AGM. We used an ex vivo system involving culturing AGM or AGM dissociated into single cells and then reaggregated into an organoid, a technique that expands HSCs (Taoudi et al., 2008; Fig. 1 B). At E11.5, the $+9.5^{+/+}$, $+9.5^{+/-}$, and $+9.5^{-/-}$ embryos were morphologically indistinguishable (Fig. 1 C). Quantitation of *Gata2* mRNA in uncultured AGMs from $+9.5^{+/+}$, $+9.5^{+/-}$, and $+9.5^{-/-}$ E11.5 embryos revealed significantly reduced *Gata2* expression in $+9.5^{-/-}$ versus $+9.5^{+/+}$ AGMs (Fig. 1 D). Whereas culturing the intact or reaggregated E11.5 AGMs for 96 h significantly induced *Gata2* expression in $+9.5^{+/+}$ AGMs, *Gata2* induction was reduced in $+9.5^{+/-}$ AGMs, and no induction was detected with $+9.5^{-/-}$ AGMs (Fig. 1 D). Thus, the +9.5 element enhances *Gata2* expression in the uncultured AGM and is essential for increased *Gata2* expression in the AGM cultures.

+9.5 element controls HSC generation in the AGM

The importance of the +9.5 element for *Gata2* expression in the AGM suggested that it might be important for AGM hematopoiesis. We quantitated erythroid/myeloid colony forming activity of E11.5 uncultured AGM and explant/reaggregate cultures. Whereas the total cells that constitute the $+9.5^{+/+}$, $+9.5^{+/-}$, and $+9.5^{-/-}$ AGMs were indistinguishable (Fig. 1 E), the homozygous mutation abolished AGM colony-forming activity (Fig. 1 F). After 96 h of culture, cell numbers were slightly higher in $+9.5^{+/+}$ versus $+9.5^{-/-}$ AGM explants (Fig. 1 G). The 96-h culture induced CFU-Cs ∼40-fold (Fig. 1, F and H). Colony-forming activity of $+9.5^{+/-}$ and $+9.5^{-/-}$ versus $+9.5^{+/+}$ cultured AGM explants/reaggregates was markedly reduced (Fig. 1 H). The +9.5 element is therefore a critical determinant of hematopoietic progenitor activity in the AGM.

To establish whether the +9.5 element requirement for progenitor activity reflects its role in the genesis and/or activity of HSCs, we transplanted $+9.5^{+/+}$, $+9.5^{+/-}$, and $+9.5^{-/-}$ E11.5-cultured AGM cells (CD45.2) into lethally irradiated recipient mice with CD45.1 spleen cells as a supporting cell population and CD45.1 bone marrow cells. At 4, 8, 12, and 16 wk after transplantation, CD45.2 cells were undetectable in peripheral blood of recipients transplanted with $+9.5^{-/-}$ AGM explants. The mean donor contribution from $+9.5^{+/+}$ AGM explants at 4, 8, 12, and 16 wk was 39.0, 61.0, 67.4, and 76.1%, respectively (Fig. 2 A). The mean contribution from $+9.5^{+/-}$ AGM explants at 4, 8, 12, and 16 wk was 25.7, 31.6, 24.0, and 25.4%, respectively. Consistent with the primary transplant analysis, secondary transplantation with bone marrow cells from the primary recipient mice revealed significantly reduced HSC activity in the $+9.5^{+/-}$ versus $+9.5^{+/+}$ donors (Fig. 2 B). Though long-term repopulating activity was reduced significantly in $+9.5^{+/-}$ versus $+9.5^{+/+}$ donors, HSCs from these donors contributed similarly to myeloid and lymphoid lineages in peripheral blood (Fig. 2 C). As HSC activity was undetectable in the $+9.5^{-/-}$ mutant AGMs, the +9.5 element is essential for generating functional HSCs in the AGM.

The ablation of HSC repopulating activity in the $+9.5^{-/-}$ mutant AGMs might reflect a +9.5 element requirement for hemogenic endothelium to generate HSCs or a requirement to expand and/or confer survival subsequent to HSC generation. Because hemogenic endothelium generates HSCs that reside in clusters intimately associated with the hemogenic endothelium, we performed whole-mount, three-dimensional embryo immunostaining to visualize HSC genesis in $+9.5^{+/+}$ and $+9.5^{-/-}$ AGMs. As previously described (Yokomizo et al., 2012), CD31 expression marks all endothelial and hematopoietic cluster cells, whereas c-Kit marks hematopoietic clusters, but not endothelial cells. Imaging of E10.5 embryos revealed $CD31^{+}$c-Kit^{+} clusters in the $+9.5^{+/+}$ dorsal aorta, whereas no clusters were apparent with the $+9.5^{-/-}$ embryos (Fig. 2, D and E; and Videos 1 and 2). Quantitative analysis of the whole dorsal aorta revealed 460 ± 21 c-Kit^{+} cells in the $+9.5^{+/+}$ dorsal aorta, versus <10 c-Kit^{+} cells in the $+9.5^{-/-}$ dorsal aorta (Fig. 2 F). The absence of c-Kit^{+} cluster cells in the $+9.5^{-/-}$ dorsal aorta and the ablation of HSC repopulating activity indicate that the +9.5 element is required for hemogenic endothelium to generate HSCs in the AGM.

+9.5 element instigates a stem cell–regulatory genetic network

In principle, the +9.5-dependent genetic network should reveal clues regarding the mechanism of the HSC deficiency in $+9.5^{-/-}$ AGM. We used RNA-seq to define the $+9.5^{+/+}$ and $+9.5^{-/-}$ AGM explant transcriptomes, which identified a cohort of significantly down-regulated genes and a smaller number of up-regulated genes in the $+9.5^{-/-}$ AGMs (FDR < 0.05; Fig. 3, A and B). Gene ontology analysis of the down-regulated cohort revealed a significant enrichment of genes involved in hematopoiesis (Fig. 3 C), including a large ensemble of genes encoding factors that control HSC development/function (Fig. 3, D and E). Genes implicated in the HSC niche were unaltered (Fig. 3, D and E), indicating that an important component of +9.5 element function is the cell autonomous induction of HSCs in the AGM. Genes encoding components of the hematopoietic-regulatory Notch pathway, which is implicated in *Gata2* regulation (Guiu et al., 2013), as well as BMP4 and Wnt signaling pathways, were also unaffected (Table S1). Consistent with the loss of HSC and progenitor activities, a host of lineage-specific genes were down-regulated. We compared the transcriptional profile of the AGM with the profile from PECAM-1^{+} cells isolated from E12.5 embryos, which we described previously (Johnson et al., 2012). Of the 44 down-regulated genes in $+9.5^{-/-}$ $PECAM^{+}$ cells, 34 were down-regulated in $+9.5^{-/-}$ AGM; 10 of the 44 down-regulated genes in $+9.5^{-/-}$ $PECAM^{+}$ cells were not altered in the $+9.5^{-/-}$ AGM, and the vast majority of the down-regulated genes in the AGM were not down-regulated in the PECAM-1^{+} cells. Thus, the +9.5 element instigates a genetic network consisting of known regulators of

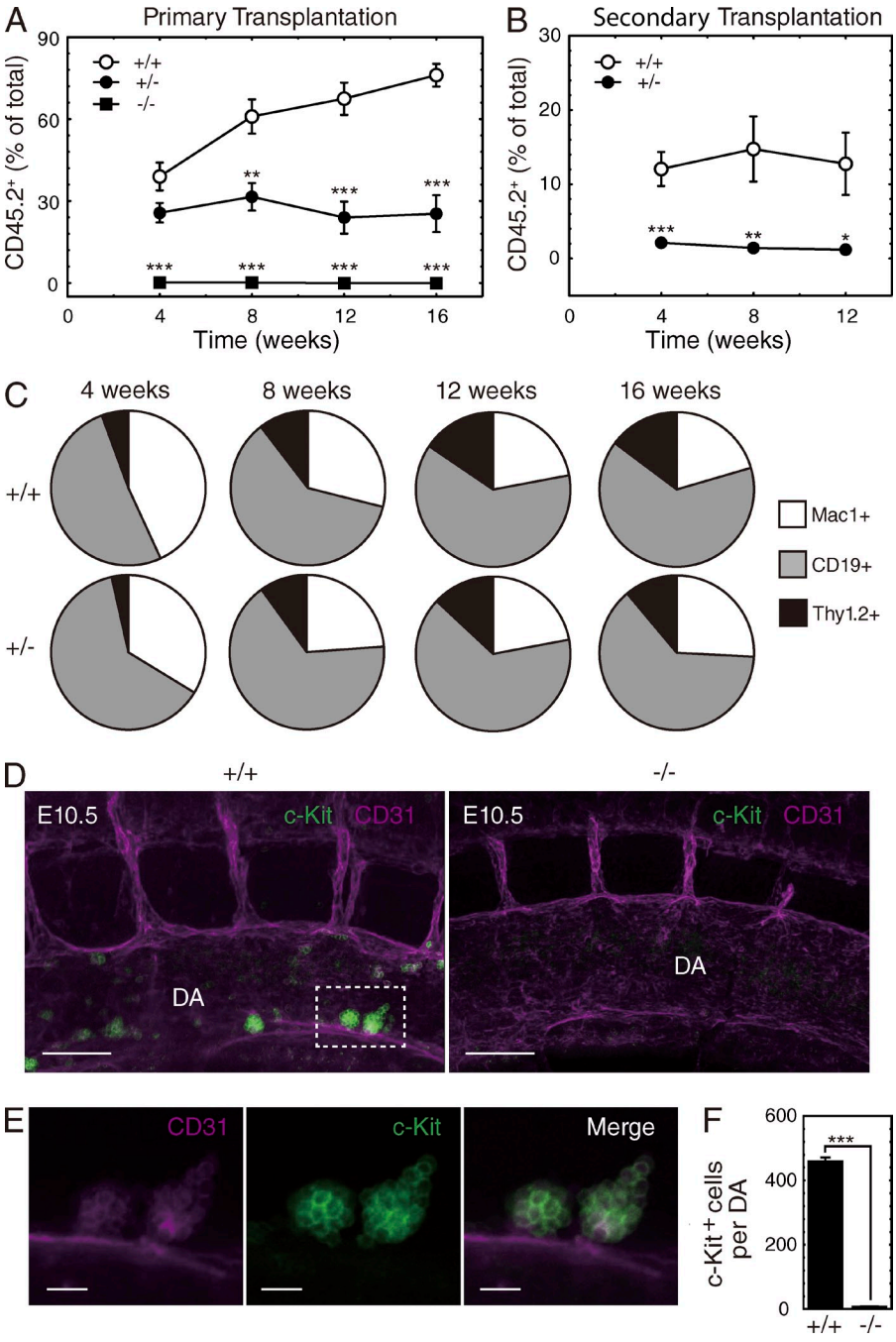

Figure 2. Absence of long-term repopulating HSC activity and HSC generation in +9.5$^{-/-}$ AGM. (A) Contribution from +9.5$^{+/-}$ and +9.5$^{-/-}$ versus +9.5$^{+/+}$ AGM explants (in a competitive transplantation assay +9.5$^{+/+}$ [n = 11]; +9.5$^{+/-}$ [n = 11]; +9.5$^{-/-}$ [n = 6]). (B) Secondary transplant with bone marrow cells from primary recipient mice (+9.5$^{+/+}$ [n = 8]; +9.5$^{+/-}$ [n = 8]). (C) The contribution of +9.5$^{+/+}$ and +9.5$^{+/-}$ donor-derived CD45.2 cells to peripheral myeloid cells (Mac1$^+$), B cells (CD19$^+$) and T cells (Thy1.2$^+$). (D) Whole-mount immunostaining of E10.5 +9.5$^{+/+}$ (left) and +9.5$^{-/-}$ (right) embryos showing CD31$^+$ cells (magenta) and c-Kit$^+$ cells (green) within the aorta region. Bar, 100 µm. (E) Higher magnification of boxed region in D showing the representative aortic hematopoietic clusters in +9.5$^{+/+}$ embryos. Bar, 20 µm. (F) Quantitation of c-Kit$^+$ cells within the whole dorsal aorta (2 litters: +9.5$^{+/+}$ [n = 3]; +9.5$^{-/-}$ [n = 3]). Error bars represent SEM. *, P < 0.05; **, P < 0.01; ***, P < 0.001 (two-tailed unpaired Student's t test). Related to Videos 1 and 2.

hematopoiesis and genes not implicated previously in controlling hematopoiesis.

Mechanism of HSC emergence in the AGM

Besides hematopoietic cell expression, GATA-2 is expressed in additional specialized cell types, including endothelial cells. GATA-2 function in endothelial cells is linked to angiogenesis, inflammation, and vascular integrity (Mammoto, 2009; Linnemann et al., 2011; Johnson et al., 2012). We asked whether the +9.5 element regulates *Gata2* expression in hematopoietic and endothelial cells within the AGM, and whether the +9.5-dependent genetic network is similar or distinct in these cell types. Sorting endothelial (CD31$^+$c-Kit$^-$) and hematopoietic cells (CD31$^+$c-Kit$^+$) from cultured AGM explants (Fig. 4 A) revealed a 1.8- and 9.5-fold reduction in endothelial and hematopoietic cells, respectively, in the +9.5$^{-/-}$ versus +9.5$^{+/+}$ AGM explants (Fig. 4 B). We quantitated expression of *Gata2* and two classes of +9.5 element-up-regulated genes identified in our RNA-seq analysis (genes required for HSC long-term repopulating activity (Rossi et al., 2012; Fig. 4 C); and genes not implicated previously in controlling HSCs [Fig. 4 D]) in the endothelial and hematopoietic

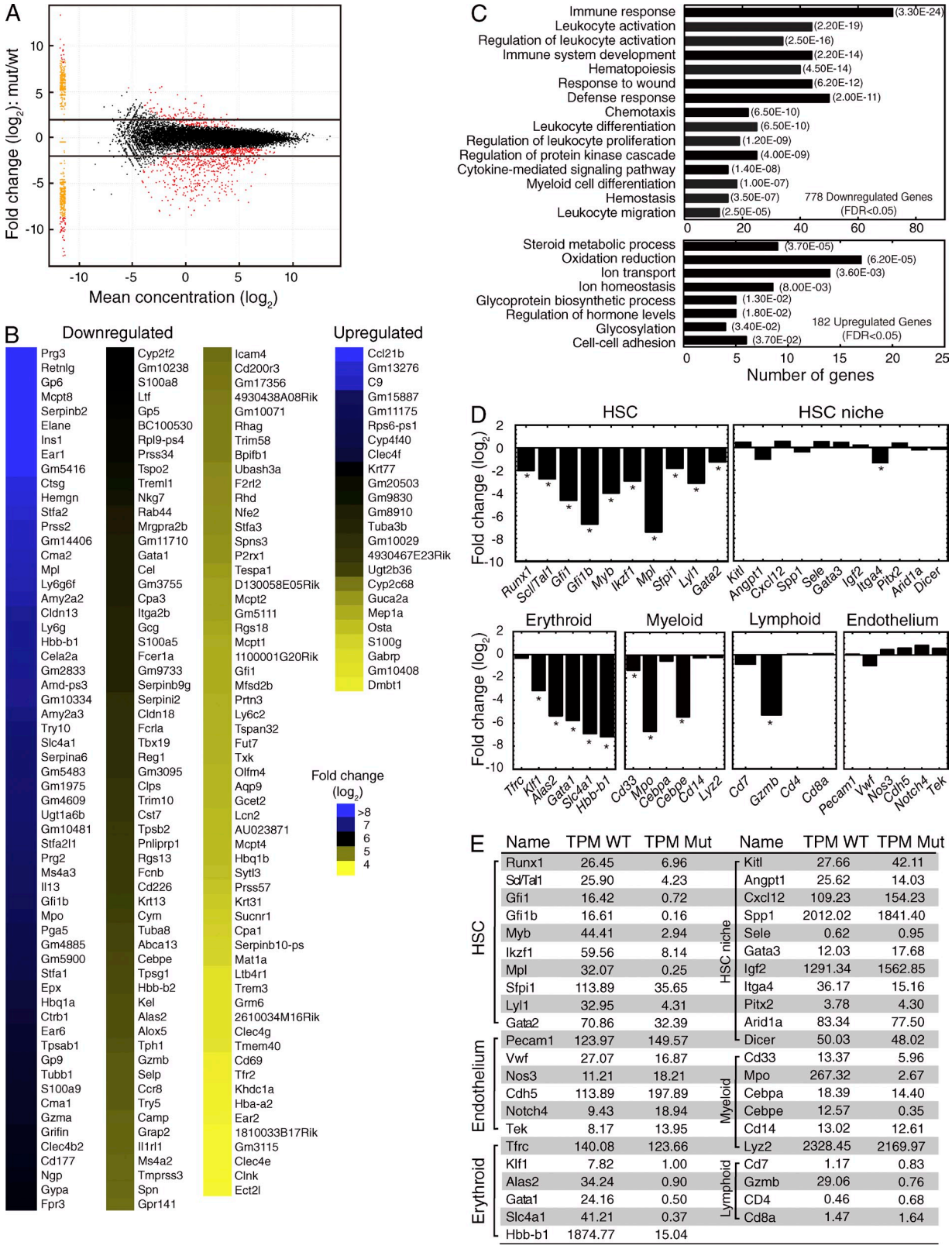

Name	TPM WT	TPM Mut	Name	TPM WT	TPM Mut
HSC			HSC niche		
Runx1	26.45	6.96	Kitl	27.66	42.11
Scl/Tal1	25.90	4.23	Angpt1	25.62	14.03
Gfi1	16.42	0.72	Cxcl12	109.23	154.23
Gfi1b	16.61	0.16	Spp1	2012.02	1841.40
Myb	44.41	2.94	Sele	0.62	0.95
Ikzf1	59.56	8.14	Gata3	12.03	17.68
Mpl	32.07	0.25	Igf2	1291.34	1562.85
Sfpi1	113.89	35.65	Itga4	36.17	15.16
Lyl1	32.95	4.31	Pitx2	3.78	4.30
Gata2	70.86	32.39	Arid1a	83.34	77.50
Endothelium			Dicer	50.03	48.02
Pecam1	123.97	149.57	Myeloid		
Vwf	27.07	16.87	Cd33	13.37	5.96
Nos3	11.21	18.21	Mpo	267.32	2.67
Cdh5	113.89	197.89	Cebpa	18.39	14.40
Notch4	9.43	18.94	Cebpe	12.57	0.35
Tek	8.17	13.95	Cd14	13.02	12.61
Erythroid			Lyz2	2328.45	2169.97
Tfrc	140.08	123.66	Lymphoid		
Klf1	7.82	1.00	Cd7	1.17	0.83
Alas2	34.24	0.90	Gzmb	29.06	0.76
Gata1	24.16	0.50	CD4	0.46	0.68
Slc4a1	41.21	0.37	Cd8a	1.47	1.64
Hbb-b1	1874.77	15.04			

Figure 3. A rich stem cell–regulatory genetic network controlled by a composite cis-element. RNA-seq-based comparison of gene expression in E11.5 +9.5$^{+/+}$ (n = 3) and +9.5$^{-/-}$ (n = 3) cultured AGM explants. (A) MA plot for +9.5$^{-/-}$ versus +9.5$^{+/+}$ cultured AGM explants. The red points indicate 778 and 182 genes down- or up-regulated (FDR < 0.05), respectively, in the mutants. (B) Heatmap depicting statistically significant, differentially expressed genes down- or up-regulated by >16 fold. (C) Gene Ontology analysis of genes down- or up-regulated in +9.5$^{-/-}$ cultured AGM explants with

cell populations from +9.5$^{+/+}$ AGM explants. The latter group was selected based on one or more of the following parameters: (a) expression in hematopoietic stem and/or progenitor cells, derived from mining BioGPS data; (b) not implicated previously in regulating hematopoiesis in the AGM; (c) expression pattern resembling *Gata2* during murine erythroid cell maturation (Kingsley et al., 2013). *c-Kit* expression was high and low in hematopoietic and endothelial cells, respectively. The other genes were either expressed higher in the endothelial or hematopoietic populations or equivalently in the two populations (Fig. 4, C and D). Comparison of expression in +9.5$^{+/+}$, +9.5$^{+/-}$, and +9.5$^{-/-}$ AGM explants revealed the +9.5 element deletion reduced *Gata2* expression in both populations (Fig. 4 E). Intriguingly, the deletion differentially affected genetic networks in the two contexts (Fig. 4, E and F). *Scl/TAL1* expression declined only in hematopoietic cells. *Scl/TAL1* is required for the genesis of HSCs and for erythroid and megakaryocytic differentiation, but not for HSC engraftment, self-renewal and myeloid and lymphoid differentiation (Mikkola et al., 2003). *Lyl1* expression declined only in endothelial cells. *Lyl1* functions redundantly with *Scl/TAL1* to maintain adult HSCs (Souroullas et al., 2009). Expression of *Runx1*, which controls the hemogenic endothelium to HSC transition (Chen et al., 2009) declined in endothelial and hematopoietic cells, but to a much greater extent in endothelial cells. Expression of the 20 genes down-regulated in the mutant explants was reduced in endothelial cells (*Lyl1*, *Ikzf1*, *Sfpi1*, and *Bex6*), hematopoietic cells (*Scl/TAL1*), or both (*Gata2*, *Myb*, *Mpl*, *Gfi1*, *Gfi1b*, *Runx1*, *Gpr56*, *Mfsd2b*, *Slc35d3*, *Fcho1*, *Lin28b*, *Gpr65*, *Hhex*, *Mmrn1*, and *Cdk6*). In a surrogate hematopoietic system (Fujiwara et al., 2009), GATA-2 occupied most of these genes (unpublished data). As certain hematopoietic genes, including *CD14* and *Hbb-y*, were unaffected by the +9.5 element deletion, perturbations of the +9.5 element-dependent genetic network did not reflect quantitative depletion of all hematopoietic cells.

Analogous to the +9.5 site activity to regulate gene expression in both the endothelial and hematopoietic cell populations, Ki67 staining analysis indicated that the +9.5 site regulated cell proliferation in both populations, but in a qualitatively different manner. The +9.5 site enhanced proliferation in the endothelial cell population (Fig. 4 G), whereas it contributed to the maintenance of quiescence in the hematopoietic cell population (Fig. 4 H). Annexin V and PI staining revealed the +9.5 site deletion induced apoptosis in both populations (Fig. 4, I and J), and therefore the +9.5 site confers survival.

The +9.5 element instigates a genetic network consisting of established HSC regulators not known to be co-regulated by any factor; genes implicated in hematopoiesis, but poorly studied in this context (*Gpr56* [Saito et al., 2013]; *Hhex*]Paz et al., 2010]; and *Cdk6* [Malumbres et al., 2004]); and genes not linked previously to hematopoiesis (e.g., *Bex6* and *Mfsd2b*). Targeted deletions of genes encoding the known HSC-regulatory components impair HSC long-term repopulating activity (Rossi et al., 2012), and therefore the simultaneous loss of multiple components is particularly catastrophic for hematopoiesis and embryonic development. Our analysis links *Gpr56* (seven-transmembrane receptor), *Hhex* (homeodomain transcription factor), and *Cdk6* (cell cycle-regulatory kinase) and additional genes to established determinants of HSC genesis/activity (Rossi et al., 2012). It is attractive to propose that they also function nonredundantly to control the genesis/activity of HSCs in vivo. Database mining revealed *Gpr56*, *Hhex*, and *Cdk6* expression is enriched in murine HSCs, common myeloid progenitors, and granulocyte macrophage progenitors (*Cdk6* only; BioGPS.org). During erythropoiesis, expression of these genes is indistinguishable from *Gata2*, with expression high in proerythroblasts and repressed thereafter (Kingsley et al., 2013). The GATA-2-like expression pattern and +9.5-dependent regulation suggest that these genes are important constituents of the +9.5-dependent genetic network.

Our results describe a novel genetic mechanism that controls development of the adult hematopoietic system in the mammalian embryo. A composite cis-regulatory element induces *Gata2* expression and is essential for HSC emergence in the AGM. This element is not required for *Gata2* expression and hematopoiesis in the yolk sac (Johnson et al., 2012). The +9.5$^{-/-}$ AGM is not competent to generate HSCs, and therefore HSCs become limiting and cannot populate the fetal liver (Fig. 4 K). The +9.5 element regulates select genes in hemogenic endothelium, distinct genes in hematopoietic precursor cell progeny, and additional genes in both cell types. Through endothelial cell-selective, hematopoietic cell–selective, and shared actions, the +9.5 element–instigated genetic network induces the emergence of stem cells that establish/maintain the adult blood system. Importantly, as the +9.5 element confers *Runx1* expression, and *Runx1* promotes the hemogenic endothelium to HSC transition, our results support a model in which the +9.5 element functions upstream of *Runx1* in this crucial process.

The results described herein illustrate the extraordinary importance of a cis-regulatory element for stem cell biology, and we predict that the +9.5 element is a foundational member of a cis-regulatory element ensemble (HSC cistrome), which nonredundantly controls HSC genesis/activity. Given the significantly reduced HSC/progenitor levels in the +9.5$^{+/-}$ AGM, the mechanistic insights described herein will be instructive vis-à-vis unraveling the molecular underpinnings

a cut-off FDR <0.05 using DAVID Bioinformatics Program (http://david.abcc.ncifcrf.gov/). The most enriched biological processes are shown with corresponding P values. (D) RNA-seq-based analysis of the expression levels of representative genes expressed in HSCs and the HSC niche that regulate hematopoiesis, as well as genes expressed in endothelium, erythroid, myeloid, and lymphoid cells (*, FDR < 0.05). (E) The relative expression levels (TPM, transcripts per million) of representative genes shown in the figure.

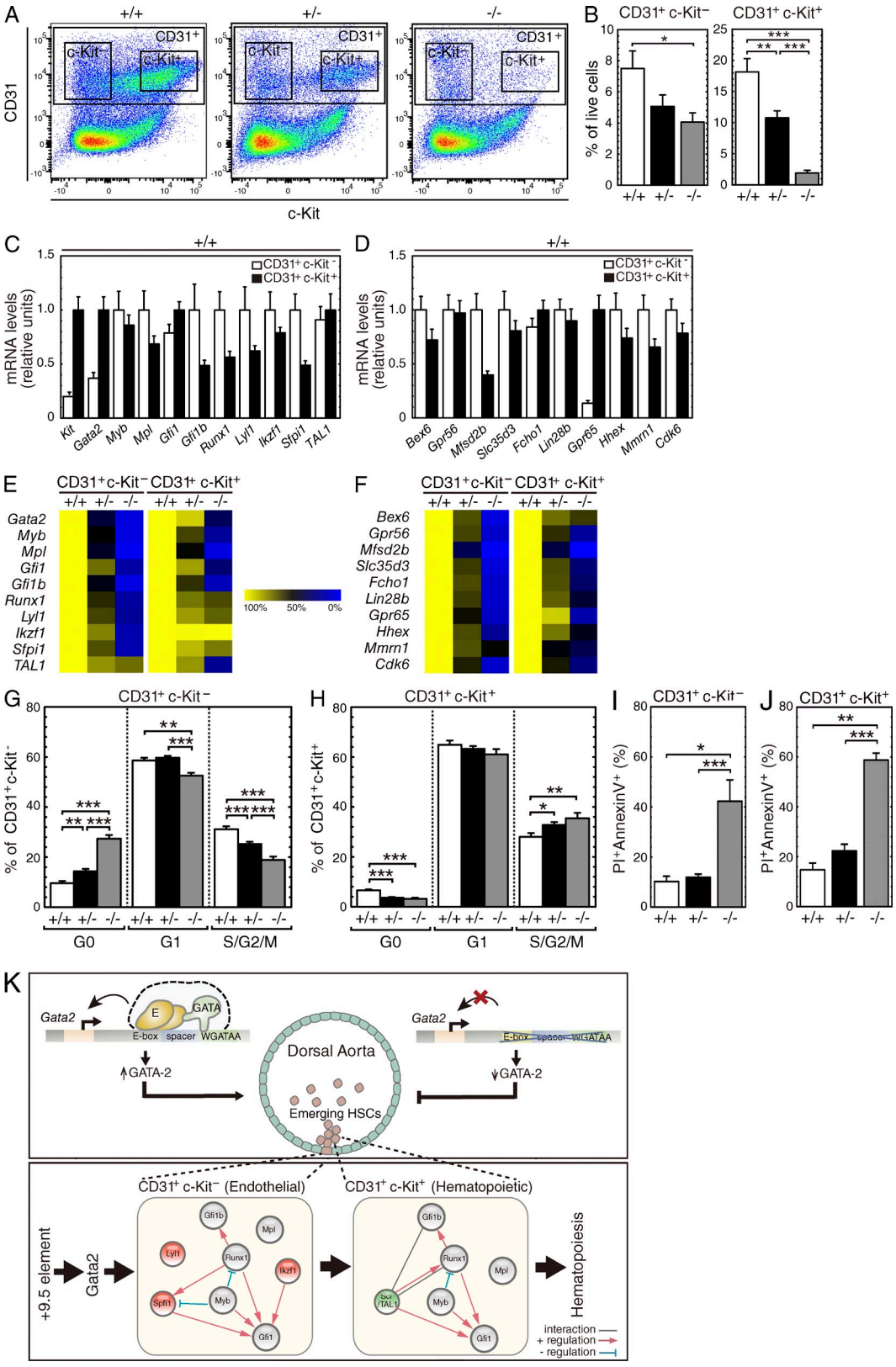

Figure 4. +9.5 element–regulated genetic network controls HSC emergence from hemogenic endothelium. (A) Representative flow cytometric plots depicting endothelial (CD31$^+$c-Kit$^-$) and hematopoietic (CD31$^+$c-Kit$^+$) cells in cultured AGM explants. (B) Quantitative analysis of flow cytometry data expressed as percentage of live cells from cultured AGM explants (2 independent experiments and 4 litters: +9.5$^{+/+}$ [n = 14]; +9.5$^{+/-}$ [n = 17]; +9.5$^{-/-}$ [n = 7]). (C and D) Quantitation of relative expression of HSC-related genes and representative novel genes in endothelial cells and hematopoietic

of MonoMAC syndrome and the associated myelodysplastic syndrome and acute myeloid leukemia (Hsu et al., 2011; Johnson et al., 2012).

MATERIALS AND METHODS

Mice and embryo generation. *Gata2* $+9.5^{+/-}$ mice generated via homologous recombination in ES cells were described previously (Johnson et al., 2012). E11.5 embryos were obtained from timed matings between *Gata2* $+9.5^{+/-}$ males and females, with the day of vaginal plug detection considered as day 0.5. Pregnant females were euthanized with CO_2, and fresh embryos were transferred into cold PBS for dissection. All animal experiments were performed with the ethical approval of the AAALAC International (Association for the Assessment and Accreditation of Laboratory Animal Care) at the University of Wisconsin-Madison.

AGM explant culture. E11.5 AGMs were dissected (Morgan et al., 2008) and cultured as previously described (Taoudi et al., 2008). In brief, intact AGMs were cultured for 4 d on Durapore filters (Millipore) at the air–liquid interface in IMDM$^+$ Media (Iscove's modified Dulbecco's media [IMDM; Invitrogen] supplemented with 20% FBS [Gemini], 4 mM L-glutamine [Invitrogen], 1% penicillin/streptomycin [Invitrogen], 0.1 mM mercaptoethanol, 100 ng/ml IL-3 [R&D Systems], 100 ng/ml Flt3L [R&D Systems], and 1.5% conditioned medium from a kit ligand-producing CHO cell line).

AGM reaggregate culture. AGMs were dissociated and reaggregated for culturing as previously described (Taoudi et al., 2008). A single-cell suspension of AGM cells was drawn into a 200-µl pipette tip. The tip containing the cell suspension was blocked with Parafilm and centrifuged in a 15-ml centrifuge tube at 300 g for 5 min. After removing the Parafilm, the reaggregate was extruded onto the Durapore filter and cultured at the air-liquid interface in IMDM$^+$ media for 4 d. AGM reaggregates, as well as whole AGM explants, were cultured in a humidified incubator at 37°C with 5% carbon dioxide. Uncultured AGMs and cultured AGM explants/reaggregates were digested in 0.1% collagenase in PBS containing 10% FBS at 37°C for 30 min and then dissociated by passing through a 27-G needle. Dissociated AGM cells were subjected to colony assay, transplantation assay, flow cytometry, and cell sorting.

Colony assay. All dissociated cells from E11.5 uncultured AGMs, or 10,000 cells from E11.5 cultured AGM explants/reaggregates, were plated in MethoCult M03434 complete media (StemCell Technologies) in a 35-mm dish. After incubation in a humidified incubator at 37°C with 5% carbon dioxide for 7 d, colonies were visualized by microscopy and quantitated.

Transplantation assay. Adult C57BL/6 recipient mice (CD45.1$^+$; 6–8 wk old) were lethally irradiated with 2 doses of 500 rad each from a Cesium source. Dissociated cells from E11.5 cultured CD45.2$^+$ AGM explants were combined based on their genotypes. 50,000 nucleated AGM cells were co-injected into individual irradiated CD45.1$^+$ recipient mice with 200,000 CD45.1$^+$ spleen cells as a support and 20,000 CD45.1$^+$ bone marrow cells. The transplanted recipient mice were maintained on trimethoprim/sulfamethoxazole-treated water for 2 wk. Blood was obtained from the retroorbital venous sinus regularly after transplantation for flow cytometric analysis, as previously described (Johnson et al., 2012). Directly conjugated antibodies specific for the following surface antigens were purchased from eBioscience: CD19 (eBio1D3), CD45.1 (A20), CD45.2 (104), Mac-1 (M1/70), and Thy1.2 (53–2.1).

Whole-embryo confocal microscopy. Embryos were fixed, stained, and analyzed as described previously (Yokomizo et al., 2011). Embryos were stained with anti–PECAM-1 and anti–c-Kit antibodies. The samples were mounted in a 1:2 mix of benzyl alcohol and benzyl benzoate (BABB) to increase the transparency of tissues and visualized with a Nikon A1R Confocal Microscope. Three-dimensional reconstructions were generated from Z-stacks (50–150 optical sections) using Figi software.

Quantitative real-time RT-PCR. Total RNA from uncultured or cultured AGMs was purified with TRIzol (Invitrogen). cDNA was synthesized from 1 µg purified total RNA by Moloney murine leukemia virus reverse transcription (M-MLV RT). Real-time PCR was performed with SYBR green master mix. Control reactions lacking M-MLV RT yielded little to no signal. Relative expression was determined from a standard curve of serial dilutions of cDNA samples, and values were normalized to 18S RNA expression. The sequences of primers used for RT-PCR and genotyping are provided in the supplementary information (Table S2).

RNA-seq and data analysis. RNA-seq was conducted with an Illumina HiSeq 2000 system. Total RNA was purified from cultured AGM explants from $+9.5^{+/+}$ ($n = 3$) and $+9.5^{-/-}$ ($n = 3$) embryos using TRIzol reagent (Invitrogen). Transcript quantification and differential expression were conducted using the software packages RSEM (Li and Dewey, 2011) and edgeR (Robinson et al., 2010), respectively. RSEM v1.1.21 was provided with a reference transcript set consisting of all protein coding transcripts from the Ensembl release 67 annotation of the NCBI Build 37 mouse genome assembly. Default parameters and Bowtie v0.12.8 were used for transcript quantification with RSEM. Transcript read counts were summed to produce counts at the level of gene symbols. These counts were then given as input to edgeR v3.0.0 for differential expression analysis. edgeR was run with a common dispersion model and default parameters. Gene symbols with Benjamini–Hochberg FDR values less than 0.05 were deemed to be differentially expressed between mutant and wild-type.

Flow cytometry analysis and cell sorting. Dissociated cells from cultured AGM explants were resuspended in PBS containing 2% FBS and passed through 25-µm cell strainers to obtain single-cell suspensions before antibody staining. APC-conjugated antibody CD31 (MEC13.3; BioLegend) and PE-conjugated antibody c-Kit (2B8, eBioscience) were used for flow cytometry and cell sorting. PI and Annexin V binding was used to determine apoptosis. For cell cycle analysis, cells were fixed, permeabilized, and stained with FITC-conjugated antibody against Ki67 (BD) and DAPI (Invitrogen). Flow cytometry analysis was performed on a FACS Caliber (BD) or MACSQuant Analyzer (Miltenyi Biotec). Cell sorting was performed on a FACSAria II cell sorter (BD Biosciences). All data were analyzed using FlowJo v9.0.2 software (Tree Star).

Online supplemental material. Table S1 shows the fold change of mRNA encoding the components of Notch, Wnt, and BMP4 pathways, and Table S2

cells from $+9.5^{+/+}$ AGM explants. (E and F) Heatmap showing quantitation of relative expression of HSC-related genes and novel genes in endothelial cells and hematopoietic cells from $+9.5^{+/+}$, $+9.5^{+/-}$, and $+9.5^{-/-}$ AGM explants. (G and H) Cell cycle analysis of endothelial (CD31$^+$c-Kit$^-$) and hematopoietic cells (CD31$^+$c-Kit$^+$) from $+9.5^{+/+}$, $+9.5^{+/-}$, and $+9.5^{-/-}$ AGM explants (thr3e independent experiments and 5 litters: $+9.5^{+/+}$ [$n = 10$]; $+9.5^{+/-}$ [$n = 22$]; $+9.5^{-/-}$ [$n = 11$]). (I and J) Flow cytometric analysis of the percentage of apoptotic cells (PI$^+$Annexin V$^+$) within the endothelial cells (CD31$^+$c-Kit$^-$) and hematopoietic cells (CD31$^+$c-Kit$^+$) from $+9.5^{+/+}$, $+9.5^{+/-}$, and $+9.5^{-/-}$ AGM explants (2 independent experiments and 2 litters: $+9.5^{+/+}$ [$n = 3$]; $+9.5^{+/-}$ [$n = 10$]; $+9.5^{-/-}$ [$n = 4$]). (K) Model describing +9.5 cis-element requirement for HSC emergence from AGM and +9.5 cis-element–dependent genetic networks in AGM endothelial and hematopoietic cells. Error bars represent SEM. *, $P < 0.05$; **, $P < 0.01$; ***, $P < 0.001$ (two-tailed unpaired Student's *t* test).

includes the sequences for the primers used for RT-PCR and genotyping. Video 1 and Video 2 show three-dimensional reconstructions of aorta region stained with c-Kit (green) and CD31 (magenta) antibodies at E10.5.

The authors acknowledge funding from National Institutes of Health grants DK68634 (E.H. Bresnick), DK50107 (E.H. Bresnick), HG005232 (C.N. Dewey), HG007019 (E.H. Bresnick and C.N. Dewey), CA152108 (J. Zhang), and HL113066 (J. Zhang), and support from the Carbone Cancer Center core grant CCSG P30 CA014520.

The authors declare no competing financial interests.

Submitted: 8 April 2013
Accepted: 26 September 2013

REFERENCES

Bertrand, J.Y., N.C. Chi, B. Santoso, S. Teng, D.Y. Stainier, and D. Traver. 2010. Haematopoietic stem cells derive directly from aortic endothelium during development. *Nature*. 464:108–111. http://dx.doi.org/10.1038/nature08738

Boisset, J.C., W. van Cappellen, C. Andrieu-Soler, N. Galjart, E. Dzierzak, and C. Robin. 2010. In vivo imaging of haematopoietic cells emerging from the mouse aortic endothelium. *Nature*. 464:116–120. http://dx.doi.org/10.1038/nature08764

Bresnick, E.H., H.Y. Lee, T. Fujiwara, K.D. Johnson, and S. Keles. 2010. GATA switches as developmental drivers. *J. Biol. Chem*. 285:31087–31093. http://dx.doi.org/10.1074/jbc.R110.159079

Bresnick, E.H., K.R. Katsumura, H.Y. Lee, K.D. Johnson, and A.S. Perkins. 2012. Master regulatory GATA transcription factors: mechanistic principles and emerging links to hematologic malignancies. *Nucleic Acids Res.* 40:5819–5831. http://dx.doi.org/10.1093/nar/gks281

Chen, M.J., T. Yokomizo, B.M. Zeigler, E. Dzierzak, and N.A. Speck. 2009. Runx1 is required for the endothelial to haematopoietic cell transition but not thereafter. *Nature*. 457:887–891. http://dx.doi.org/10.1038/nature07619

Dzierzak, E., and N.A. Speck. 2008. Of lineage and legacy: the development of mammalian hematopoietic stem cells. *Nat. Immunol*. 9:129–136. http://dx.doi.org/10.1038/ni1560

Fujiwara, T., H. O'Geen, S. Keles, K. Blahnik, A.K. Linnemann, Y.A. Kang, K. Choi, P.J. Farnham, and E.H. Bresnick. 2009. Discovering hematopoietic mechanisms through genome-wide analysis of GATA factor chromatin occupancy. *Mol. Cell*. 36:667–681. http://dx.doi.org/10.1016/j.molcel.2009.11.001

Grass, J.A., H. Jing, S.I. Kim, M.L. Martowicz, S. Pal, G.A. Blobel, and E.H. Bresnick. 2006. Distinct functions of dispersed GATA factor complexes at an endogenous gene locus. *Mol. Cell. Biol*. 26:7056–7067. http://dx.doi.org/10.1128/MCB.01033-06

Guiu, J., R. Shimizu, T. D'Altri, S.T. Fraser, J. Hatakeyama, E.H. Bresnick, R. Kageyama, E. Dzierzak, M. Yamamoto, L. Espinosa, and A. Bigas. 2013. Hes repressors are essential regulators of hematopoietic stem cell development downstream of Notch signaling. *J. Exp. Med*. 210:71–84. http://dx.doi.org/10.1084/jem.20120993

Hsu, A.P., E.P. Sampaio, J. Khan, K.R. Calvo, J.E. Lemieux, S.Y. Patel, D.M. Frucht, D.C. Vinh, R.D. Auth, A.F. Freeman, et al. 2011. Mutations in GATA2 are associated with the autosomal dominant and sporadic monocytopenia and mycobacterial infection (MonoMAC) syndrome. *Blood*. 118:2653–2655. http://dx.doi.org/10.1182/blood-2011-05-356352

Johnson, K.D., A.P. Hsu, M.J. Ryu, J. Wang, X. Gao, M.E. Boyer, Y. Liu, Y. Lee, K.R. Calvo, S. Keles, et al. 2012. Cis-element mutated in GATA2-dependent immunodeficiency governs hematopoiesis and vascular integrity. *J. Clin. Invest*. 122:3692–3704. http://dx.doi.org/10.1172/JCI61623

Kingsley, P.D., E. Greenfest-Allen, J.M. Frame, T.P. Bushnell, J. Malik, K.E. McGrath, C.J. Stoeckert, and J. Palis. 2013. Ontogeny of erythroid gene expression. *Blood*. 121:e5–e13. http://dx.doi.org/10.1182/blood-2012-04-422394

Li, B., and C.N. Dewey. 2011. RSEM: accurate transcript quantification from RNA-Seq data with or without a reference genome. *BMC Bioinformatics*. 12:323. http://dx.doi.org/10.1186/1471-2105-12-323

Lim, K.C., T. Hosoya, W. Brandt, C.J. Ku, S. Hosoya-Ohmura, S.A. Camper, M. Yamamoto, and J.D. Engel. 2012. Conditional Gata2 inactivation results in HSC loss and lymphatic mispatterning. *J. Clin. Invest*. 122:3705–3717. http://dx.doi.org/10.1172/JCI61619

Ling, K.W., K. Ottersbach, J.P. van Hamburg, A. Oziemlak, F.Y. Tsai, S.H. Orkin, R. Ploemacher, R.W. Hendriks, and E. Dzierzak. 2004. GATA-2 plays two functionally distinct roles during the ontogeny of hematopoietic stem cells. *J. Exp. Med*. 200:871–882. http://dx.doi.org/10.1084/jem.20031556

Linnemann, A.K., H. O'Geen, S. Keles, P.J. Farnham, and E.H. Bresnick. 2011. Genetic framework for GATA factor function in vascular biology. *Proc. Natl. Acad. Sci. USA*. 108:13641–13646. http://dx.doi.org/10.1073/pnas.1108440108

Malumbres, M., R. Sotillo, D. Santamaría, J. Galán, A. Cerezo, S. Ortega, P. Dubus, and M. Barbacid. 2004. Mammalian cells cycle without the D-type cyclin-dependent kinases Cdk4 and Cdk6. *Cell*. 118:493–504. http://dx.doi.org/10.1016/j.cell.2004.08.002

Mammoto, A., K.M. Connor, T. Mammoto, C.W. Yung, D. Huh, C.M. Aderman, G. Mostoslavsky, L.E. Smith, and D.E. Ingber. 2009. A mechanosensitive transcriptional mechanism that controls angiogenesis. *Nature*. 457:1103–1108. http://dx.doi.org/10.1038/nature07765

Medvinsky, A., and E. Dzierzak. 1996. Definitive hematopoiesis is autonomously initiated by the AGM region. *Cell*. 86:897–906. http://dx.doi.org/10.1016/S0092-8674(00)80165-8

Medvinsky, A.L., N.L. Samoylina, A.M. Müller, and E.A. Dzierzak. 1993. An early pre-liver intraembryonic source of CFU-S in the developing mouse. *Nature*. 364:64–67. http://dx.doi.org/10.1038/364064a0

Mikkola, H.K., J. Klintman, H. Yang, H. Hock, T.M. Schlaeger, Y. Fujiwara, and S.H. Orkin. 2003. Haematopoietic stem cells retain long-term repopulating activity and multipotency in the absence of stem-cell leukaemia SCL/tal-1 gene. *Nature*. 421:547–551. http://dx.doi.org/10.1038/nature01345

Morgan, K., M. Kharas, E. Dzierzak, and D.G. Gilliland. 2008. Isolation of early hematopoietic stem cells from murine yolk sac and AGM. *J. Vis. Exp.* 16:789.

Paz, H., M.R. Lynch, C.W. Bogue, and J.C. Gasson. 2010. The homeobox gene Hhex regulates the earliest stages of definitive hematopoiesis. *Blood*. 116:1254–1262. http://dx.doi.org/10.1182/blood-2009-11-254383

Robinson, M.D., D.J. McCarthy, and G.K. Smyth. 2010. edgeR: a Bioconductor package for differential expression analysis of digital gene expression data. *Bioinformatics*. 26:139–140. http://dx.doi.org/10.1093/bioinformatics/btp616

Rodrigues, N.P., V. Janzen, R. Forkert, D.M. Dombkowski, A.S. Boyd, S.H. Orkin, T. Enver, P. Vyas, and D.T. Scadden. 2005. Haploinsufficiency of GATA-2 perturbs adult hematopoietic stem-cell homeostasis. *Blood*. 106:477–484. http://dx.doi.org/10.1182/blood-2004-08-2989

Rodrigues, N.P., A.S. Boyd, C. Fugazza, G.E. May, Y. Guo, A.J. Tipping, D.T. Scadden, P. Vyas, and T. Enver. 2008. GATA-2 regulates granulocyte-macrophage progenitor cell function. *Blood*. 112:4862–4873. http://dx.doi.org/10.1182/blood-2008-01-136564

Rossi, L., K.K. Lin, N.C. Boles, L. Yang, K.Y. King, M. Jeong, A. Mayle, and M.A. Goodell. 2012. Less is more: unveiling the functional core of hematopoietic stem cells through knockout mice. *Cell Stem Cell*. 11:302–317. http://dx.doi.org/10.1016/j.stem.2012.08.006

Saito, Y., K. Kaneda, A. Suekane, E. Ichihara, S. Nakahata, N. Yamakawa, K. Nagai, N. Mizuno, K. Kogawa, I. Miura, et al. 2013. Maintenance of the hematopoietic stem cell pool in bone marrow niches by EVI1-regulated GPR56. *Leukemia*. 27:1637–1649. http://dx.doi.org/10.1038/leu.2013.75

Snow, J.W., J.J. Trowbridge, T. Fujiwara, N.E. Emambokus, J.A. Grass, S.H. Orkin, and E.H. Bresnick. 2010. A single cis element maintains repression of the key developmental regulator Gata2. PLoS Genet. 6:e1001103.

Snow, J.W., J.J. Trowbridge, K.D. Johnson, T. Fujiwara, N.E. Emambokus, J.A. Grass, S.H. Orkin, and E.H. Bresnick. 2011. Context-dependent function of "GATA switch" sites in vivo. *Blood*. 117:4769–4772.

Souroullas, G.P., J.M. Salmon, F. Sablitzky, D.J. Curtis, and M.A. Goodell. 2009. Adult hematopoietic stem and progenitor cells require either Lyl1 or

Scl for survival. *Cell Stem Cell*. 4:180–186. http://dx.doi.org/10.1016/j.stem.2009.01.001

Taoudi, S., C. Gonneau, K. Moore, J.M. Sheridan, C.C. Blackburn, E. Taylor, and A. Medvinsky. 2008. Extensive hematopoietic stem cell generation in the AGM region via maturation of VE-cadherin+CD45+ pre-definitive HSCs. *Cell Stem Cell*. 3:99–108. http://dx.doi.org/10.1016/j.stem.2008.06.004

Tsai, F.Y., G. Keller, F.C. Kuo, M. Weiss, J. Chen, M. Rosenblatt, F.W. Alt, and S.H. Orkin. 1994. An early haematopoietic defect in mice lacking the transcription factor GATA-2. *Nature*. 371:221–226. http://dx.doi.org/10.1038/371221a0

Wilson, N.K., S.D. Foster, X. Wang, K. Knezevic, J. Schütte, P. Kaimakis, P.M. Chilarska, S. Kinston, W.H. Ouwehand, E. Dzierzak, et al. 2010. Combinatorial transcriptional control in blood stem/progenitor cells: genome-wide analysis of ten major transcriptional regulators. *Cell Stem Cell*. 7:532–544. http://dx.doi.org/10.1016/j.stem.2010.07.016

Yokomizo, T., C.E. Ng, M. Osato, and E. Dzierzak. 2011. Three-dimensional imaging of whole midgestation murine embryos shows an intravascular localization for all hematopoietic clusters. *Blood*. 117:6132–6134. http://dx.doi.org/10.1182/blood-2011-02-334037

Yokomizo, T., T. Yamada-Inagawa, A.D. Yzaguirre, M.J. Chen, N.A. Speck, and E. Dzierzak. 2012. Whole-mount three-dimensional imaging of internally localized immunostained cells within mouse embryos. *Nat. Protoc.* 7:421–431. http://dx.doi.org/10.1038/nprot.2011.441

Zovein, A.C., J.J. Hofmann, M. Lynch, W.J. French, K.A. Turlo, Y. Yang, M.S. Becker, L. Zanetta, E. Dejana, J.C. Gasson, et al. 2008. Fate tracing reveals the endothelial origin of hematopoietic stem cells. *Cell Stem Cell*. 3:625–636. http://dx.doi.org/10.1016/j.stem.2008.09.018